Citation: Ibe., C.U., 2020. Geochemistry of the Precambrian Basement of the Bamenda massif of southeastern Nigeria: petrogenesis and tectonic setting. Geologica Acta, 18.19, 1-9, I-IV.
DOI: 10.1344/GeologicaActa2020.18.19

geologica acta

Geochemistry of the Precambrian Basement of the Bamenda massif of southeastern Nigeria: petrogenesis and tectonic setting

C.U. Ibe

Department of Geology, University of Nigeria
410001 Nsukka. E-mail: chinedu.ibe@unn.edu.ng. Orcid: 0000-0002-6708-3520

ABSTRACT

A trace and Rare Earth Element (REE) geochemical study of twenty samples of migmatitic banded gneisses, garnet biotite schists, dolerites, granites and rhyolites was carried out in a bid to determine their petrogenetic and tectonic significance in the evolution of the southeastern Basement complex of Nigeria. The data show that partial melting (crustal anatexis) of migmatitic gneisses and schists played a significant role in the evolution of the granitic intrusions. This is supported by a highly incompatible element ratio in the granitic intrusions (Rb/Sr= 0.16 to 1.31 and Ba/Sr= 0.75 to 6.21) compared with that of the migmatitic gneisses and schists (Rb/Sr= 0.051 to 0.824; Ba/Sr= 0.7 to 5). Higher ratios of Ba/Sr and Rb/Sr and lower values of the Ba/Rb ratio in some granitic intrusions suggest an increase in fractionation during anatexis. Partial melting also plays a role in the smooth REE patterns shown by most of these rocks and the negative Eu anomaly as indicated by the Eu/Eu* ratio (0.097 to 0.7). Light Rare Earth Element (LREE) enrichment is evident in the high ratio values of Ce/Yb_N (12.08-174.5), La/Yb_N (15.2-228.4) and La/Sm_N (2.6-7.2) in the granitic intrusions. Tectonic discrimination diagrams of the rocks indicate that basement rocks were most probably formed in a post-collision orogenic setting while dolerite and rhyolite developed in a within-plate anorogenic setting.

KEYWORDS | **Crustal anatexis. Petrogenesis. Fractionation. Tectonism. LREE enrichment.**

INTRODUCTION

The trace and Rare Earth Element (REE) characteristics of igneous rocks provide significant evidence of the origin and evolution of magmas and are useful to investigate the tectono-magmatic origin of Precambrian terranes. A simple assumption is that magmas that are generated by similar geological processes possess the same geochemical attributes. These attributes facilitate a comparison through tectonic discriminatory diagrams (*e.g.* Floyd and Winchester, 1975; Pearce and Cann, 1973; Pearce *et al*., 1984; Winchester *et al*., 1995). Although the interpretation of geochemical data for magmatic processes and the interaction of magmas with crustal materials are sometimes complex (*e.g.* Castro *et al*., 1991; Chappell, 1996; Frost and Mahood, 1987; Neves and Vauchez, 1995), geochemical data in combination with other geological evidence have proved essential for the interpretation of the petrogenesis and tectonic setting of crustal igneous provinces.

The extensive occurrence of migmatitic gneisses and migmatites as well as schists attests to the fact that crustal anataxis is a normal phenomenon. There is no consensus among researchers to date on whether or not migmatites and migmatitic gneisses represent the source regions of anatectic melts (Brown, 1994; Sawyer, 1998). Nevertheless, Sawyer (1996) reported that diatexite migmatites have some chemical and rheological properties that suggest that they are the source of granitic magmas. Lambert and Heier (1968) also reported the occurrence of granulites depleted in incompatible major and trace elements in the lower continental crust. Hence, these rocks have been considered

as refractory materials of partial melting complimenting granitic magmas (Clemens, 1990; Vielzeuf *et al*., 1990). The concentration of trace elements and REE and their distribution patterns play a major role in unraveling the petrogenesis of both granitic and basaltic rocks. They account for fractionation and resolve the question of whether granitic rocks were derived from partial melting (anatexis) or magmatic differentiation (Nockolds and Allen, 1953). Some trace elements in discrimination diagrams are often very useful indicators of tectonic setting of rocks (Pearce *et al*., 1984). In most parts of the Precambrian Basement complex of southeastern Nigeria, the rocks are predominantly gneisses, migmatitic banded gneisses of granitic to granodioritic compositions and granitic intrusions. They include paraschists with mica schists, staurolite schists, Banded Iron Formations (BIF) and marble (Anike *et al*., 1993).

The study of basement rocks in southeastern Nigeria has received very little attention to date. Few studies on trace elements and REE exist, and the most recent work in this area is by Obiora (2012), who provided the background to the present study. Other works are by Obiora and Ukaegbu (2009), Rahman *et al*. (1988), Ukaegbu and Ekwueme (2006). This study seeks to elucidate the role of the Precambrian metamorphic basement complex in the evolution of the granitic rocks forming the Bamenda massif (southeastern basement complex of Nigeria) using the trace element and REE characteristics.

GEOLOGICAL SETTING AND ROCKS

The study area lies within the Trans Saharan Orogenic Belt (TSOB) and is situated between the West African Craton, the Congo-Gabon Craton and the Tuareg Shield (Fig. 1). It is the extension of the Bamenda highlands of Cameroun into southeastern Nigeria, forming the southeastern Precambrian Basement Complex of Nigeria (Fig. 1). The rocks form a unit known as the Migmatitic Banded Gneisses (MBGn) which is composed of garnet mica schist, granitic intrusions, dolerite dykes, porphyritic

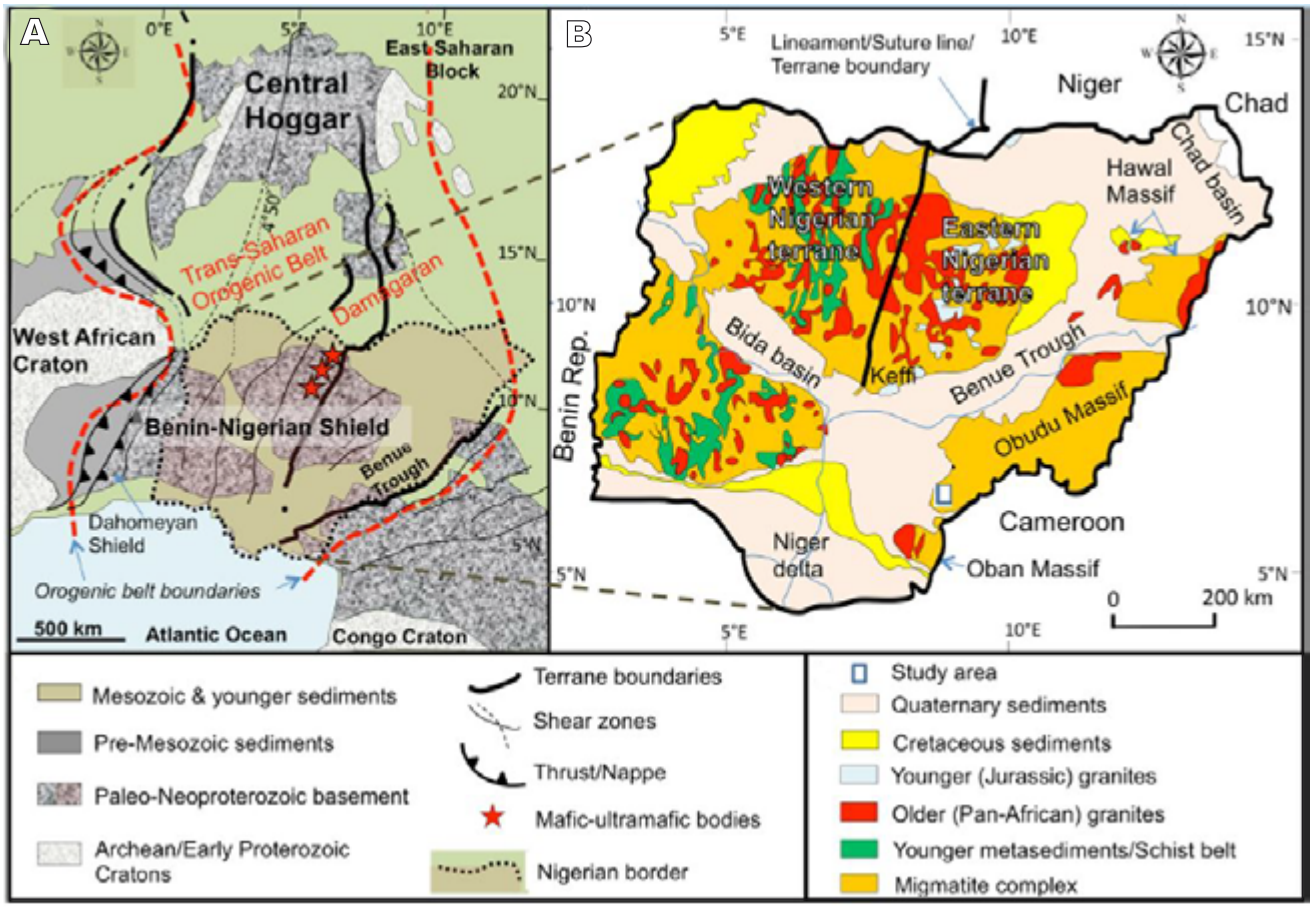

FIGURE 1. The geological map of the Hoggar-Aïr-Nigeria province showing the Neoproterozoic Trans-Saharan (Pan African) Belt resulting from terrane amalgamation between the cratons of West Africa and Congo and the East Saharan block (modified from Ugwuonah *et al*., 2017). Mobile belt boundaries adapted from Cordani *et al*. (2013). Location of study area is shown.

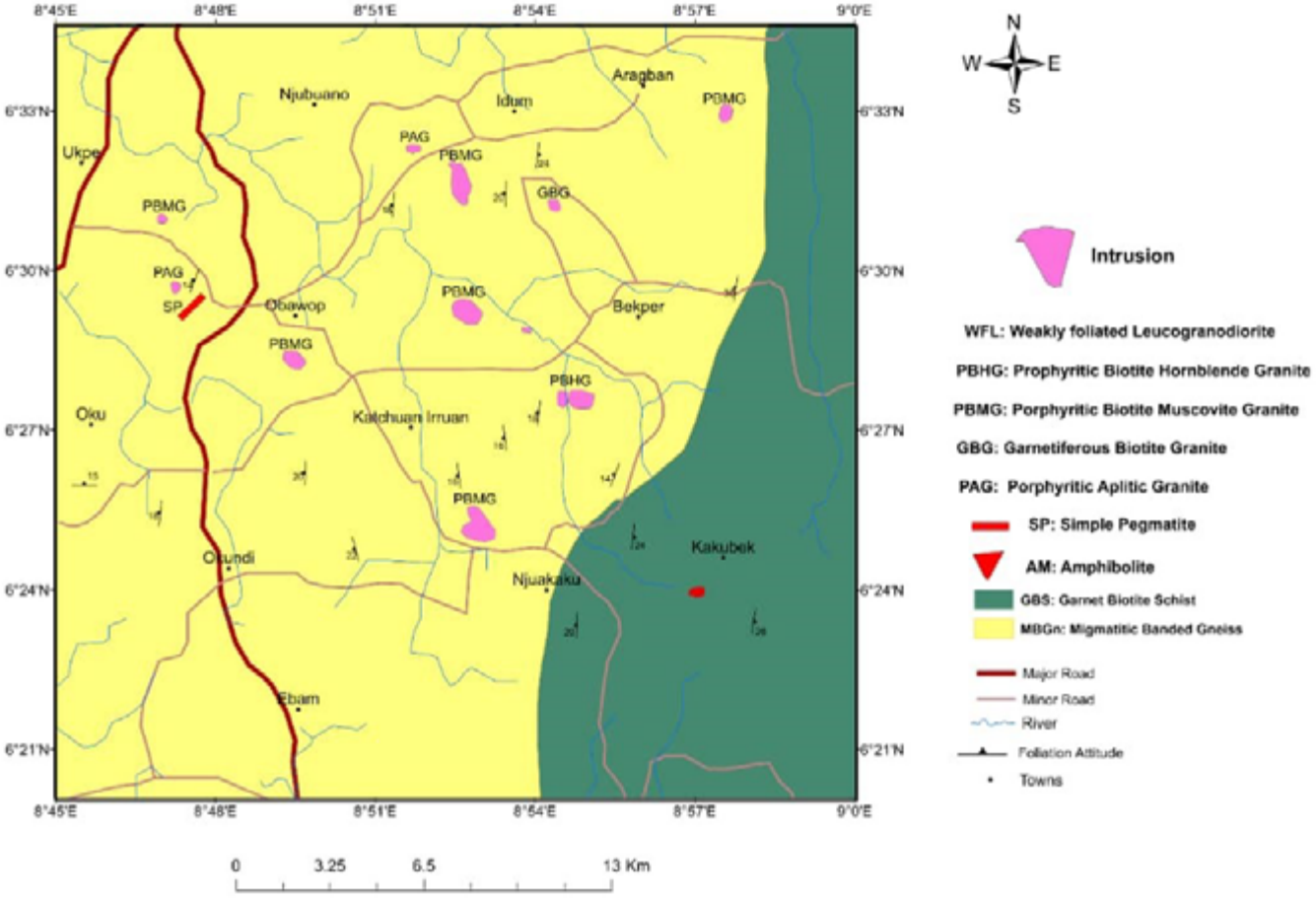

FIGURE 2. Geological map of the study area.

rhyolites and pegmatites. The granitic intrusions include Weakly Foliated Leucogranodiorite (WFL), Porphyritic Hornblende Biotite Granite (PHBG), Porphyritic Muscovite Biotite Granite (PMBG), Garnetiferous Biotite Granite (GBG), Pegmatitic Granite (PG) and Porphyritic Aplitic Granite (PAG) (Fig. 2). Detailed descriptions of these granitic rocks can be found in Ibe and Obiora (2019). The MBGn are deformed by minor folds, numerous quartzo-feldspathic veins and ptygmatic folds. Moreover, lenses of melanocratic to mesocratic micaceous schistose rocks are common in the outcrops of the granitic intrusions. These rocks occur in a low-lying unit around Bitiah in Kakwagom Irruan and have been subjected to varying degrees of weathering. The outcrop along River Rika in Katchuan Irruan has a very well-developed gneissose foliation. Furthermore, quartzo-feldspathic layers (0.2 to 0.4cm thick) alternate with gray gneissic layers of about 1.0 to 1.5cm thick. The folding of the melanocratic and leucocratic layers is very intense at this outcrop, and the melanocratic layers consist mainly of acicular hornblende. The exposure at Njuakaku hill displays intense micro-folding of quartzo-feldspathic injections and ptygmatic folds. The petrographic features of this rock unit are described in detail in Ibe (2020).

ANALITYCAL METHOD

Trace and REE concentrations of representative samples of the granitic basement complex, the dolerite dykes and the porphyritic rhyolite were determined by Inductively Coupled Plasma-Mass Spectrometry (ICP-MS) using dissolution methods. The analyses were carried out at Bureau Veritas Minerals laboratory, Perth, Western Australia. The samples were fused with sodium peroxide, and the melt was subsequently dissolved in diluted hydrochloric acid for analysis. Boron concentrations were measured using Inductively Coupled Plasma-Optical Emission Spectrometry (ICP-OES). The samples were cast using a 66:34 flux with 4% lithium nitrate added to form a glass bead. The major elements were determined by X-Ray Fluorescence Spectrometry (XRF) except for FeO, which was determined volumetrically. Loss on Ignition (LOI) was determined using a robotic Thermo-Gravimetric Analyzer

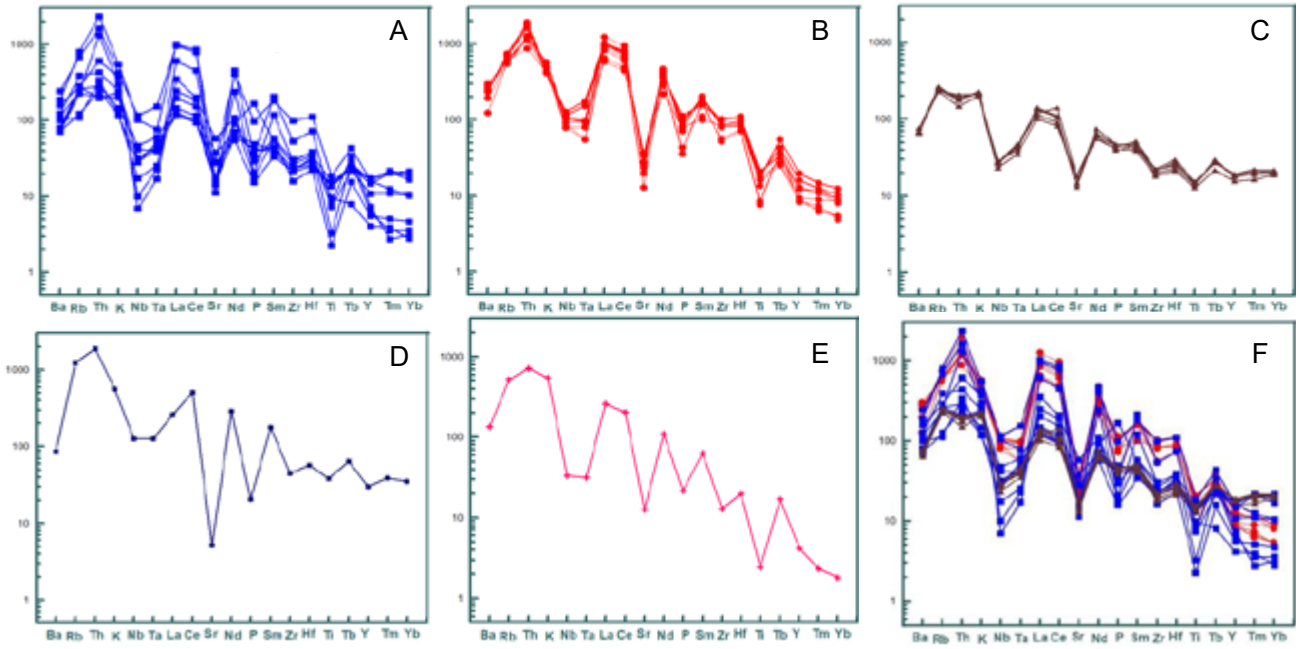

FIGURE 3. Chondrite-normalized spidergrams: A) migmatitic banded gneisses; B) granitic intrusions; C) garnet mica schist; D) dolerites; E) rhyolite porphyry; F) A, B and C combined. Values from Thompson (1982).

(TGA) system. Temperature in the furnace varied between 110 and 1000ºC.

RESULTS

Trace element and REE concentrations in the rocks are presented in Tables I and II respectively. The trace element concentrations in average granite and crust (Taylor, 1965), average diabase (Wang *et al*., 2004) and average porphyritic rhyolite (Singh *et al*., 2006) are shown in Table I for comparison. The REE data were normalized using the chondrite values of Sun and McDonough (1991). The granitic rocks consist mainly of quartz, microcline, plagioclase, orthoclase, muscovite, as well as garnet and biotite as the mafic mineral fraction. Modal and normative hypersthene and corundum are common constituents of these rocks (Ibe and Obiora, 2019).

Trace element concentrations

The High Field Strength Elements (HFSE) (U, Sn, Zr, Nb, Ta) and Large Ion Lithophile Elements (LILE) (Rb, Cs, Ba Pb, Sr, Th and REE) are of the same magnitude as in average granite and crust. The spider diagram of the samples (Fig. 3A-F) shows the dominance of HFSE and LILE. Migmatitic gneiss and some of the granitic intrusions are enriched in Nb (7.4 to 40.3ppm), Sn (0.8 to 4.8ppm) and Th (3.7 to 68.4ppm). Of all the elements of the first transition series (atomic number 21 to 30), Ni and Cr show abnormally high values compared with average granite and crust. The values of Ni range from 8 to 98ppm in the migmatitic gneiss and schists and 1 to 90ppm in the granitic intrusions; Cr ranges from 14 to 161ppm and 0 to 120ppm in the two rock types, respectively. Dolerite are enriched in Rb, Th and Ce whereas porphyritic rhyolite is depleted in Nb, Ta, Ba and Sr. The Rb/Sr ratios are 0.051 to 0.824 in the migmatitic gneiss and schist; 0.16 to 1.31 in the granitic intrusions; 0.38 to 7.03 in the dolerite and 0.8 in the porphyritic rhyolite. In Figure 3F, the spidergram shows that the migmatitic gneisses, schists and granitic rocks display an almost perfect overlap in the concentrations of elements. The Ba/Rb ratios are 5.6 to 18.01 in the migmatitic gneiss and schist; 4.32 to 10.1 in the granitic intrusions; 1.38 to 7.05 in the dolerite and 6.19 in the porphyritic rhyolite. Unlike the Rb/Sr ratios, the Ba/Rb ratios are higher in the granitic intrusions than in the biotite depleted intrusions. The Ba/Sr ratios range from 0.7 to 5 in the migmatitic gneiss and schist; 0.75 to 6.21 in the granitic intrusion; 2.6 to 9.7 in the dolerite and 4.92 in the porphyritic rhyolite. Generally, the Rb/Sr and the Ba/Sr ratios are higher in the granitic intrusions than in the migmatitic gneisses and schists whereas the Ba/Rb ratios are lower.

Plots of the granitic rocks in the Rb versus (Y+Nb) discrimination diagram (Pearce *et al*., 1984) and the Rb/30-Hf-3Ta ternary diagram of Harris *et al*. (1986) the granitic rocks plot within post-collisional setting (Fig. 4), whereas in the Zr/Y versus Zr diagram of Pearce and Norry (1979) (Fig. 5), dolerite is present in the field of within-plate-

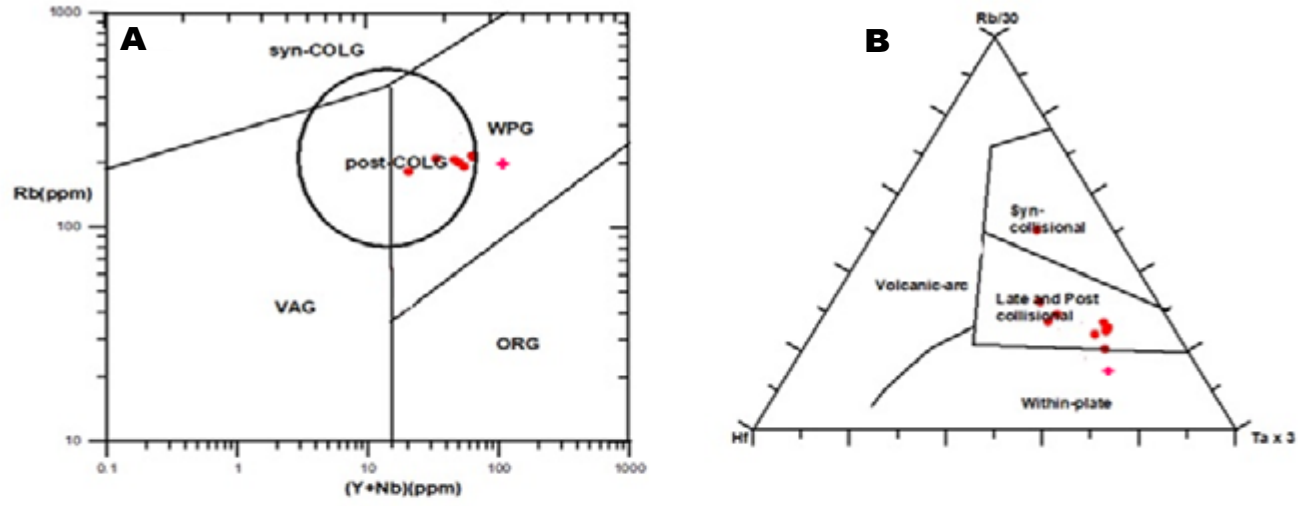

FIGURE 4. A) Post collisional characterization of the granitoids shown in the Rb versus Y+Nb diagram of Pearce *et al.*, 1984. B) Plots of the rocks in the fields of Syn-collisional to Late/post-collisional granitoids on the Rb/30 Hf (Ta x 3) ternary diagram of Harris *et al.* (1986). Syn- COLG= syn-collision granites; post-COLG= post-collision granites; WPG= within plate granites; VAG= volcanic arc granites; ORG= ocean ridge granites.

basalt. In the Rb versus (Y+Nb) diagram of Pearce *et al.* (1984) (Fig. 4), porphyritic rhyolite, in contrast, is in the intra-plate-granite setting.

REE concentrations and patterns

Generally, all the rocks are enriched in Light Rare Earth Elements (LREE) with respect to the Heavy Rare Earth Elements (HREE). The highest values of the enrichment factor given by the LREE/HREE ratio are shown by the migmatitic gneiss (36.6), porphyritic granites (40.35), rhyolite porphyry (54.59) and dolerites (36.82).

The REE concentration in the rocks shows four distinct patterns (Fig. 6). The migmatitic banded gneisses display a downward sloping LREE pattern with a very slight negative Eu anomaly and an almost flat HREE (Fig. 6A). The garnet mica schist pattern (Fig. 6C) is an exact replica of the migmatitic gneisses (Fig. 6F). All the granites show a sloping pattern with a strong Eu depletion (Fig. 6B). The rhyolite porphyry shows a concave upward pattern with a mild Eu anomaly (Fig. 6E) whereas the pattern in the dolerite is almost flat with a strong negative Eu anomaly (Fig. 6D).

As for the quantitative measures of the Eu anomaly, the Eu/Eu ratio is less than 1 for all the granitic rocks, which means that they all have a negative Eu anomaly, while it is above 1 for some migmatitic gneisses and schists. The porphyritic rhyolite, porphyritic muscovite biotite granite and the porphyritic hornblende biotite granite have a higher negative Eu anomaly than the other rocks (0.3, 0.2 and 0.2). The normalized ratios of La to Yb (*i.e.* La_N/Yb_N) range from 5.6 to 93.1 in the migmatitic gneisses and schists; 1.2 to 183.6 in the granites; 1.96 to 7.3 in the dolerites and 228.4 in the rhyolite porphyry. The Ce_N/Yb_N and La_N/Sm_N ratios follow the same trend than the La_N/Yb_N ratios.

DISCUSSION

The Ba/Rb ratios in the granitic intrusions (4.32 to 10.1) are lower than in the migmatitic gneisses (5.6 to 18.01). This suggests fractionation trends during partial

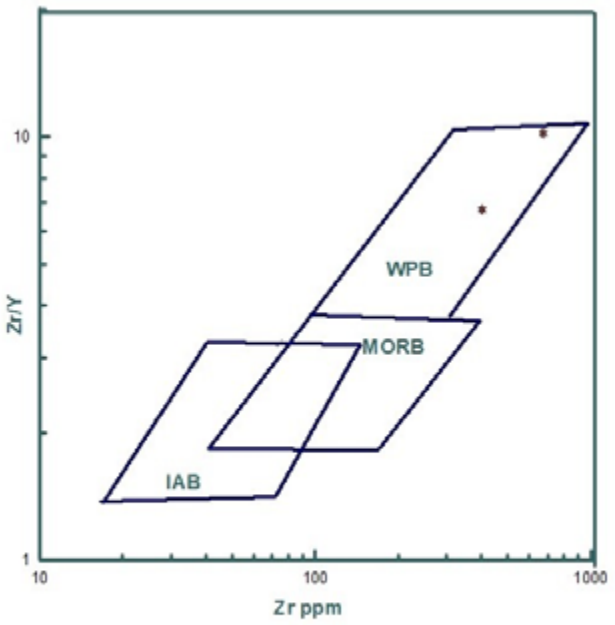

FIGURE 5. Zr/Y ratio versus Zr diagram of Pearce and Norry (1979) showing the dolerites in the WPB field. WPB= within plate basalt; MORB= mid oceanic ridge basalt; IAB= island arc basalt.

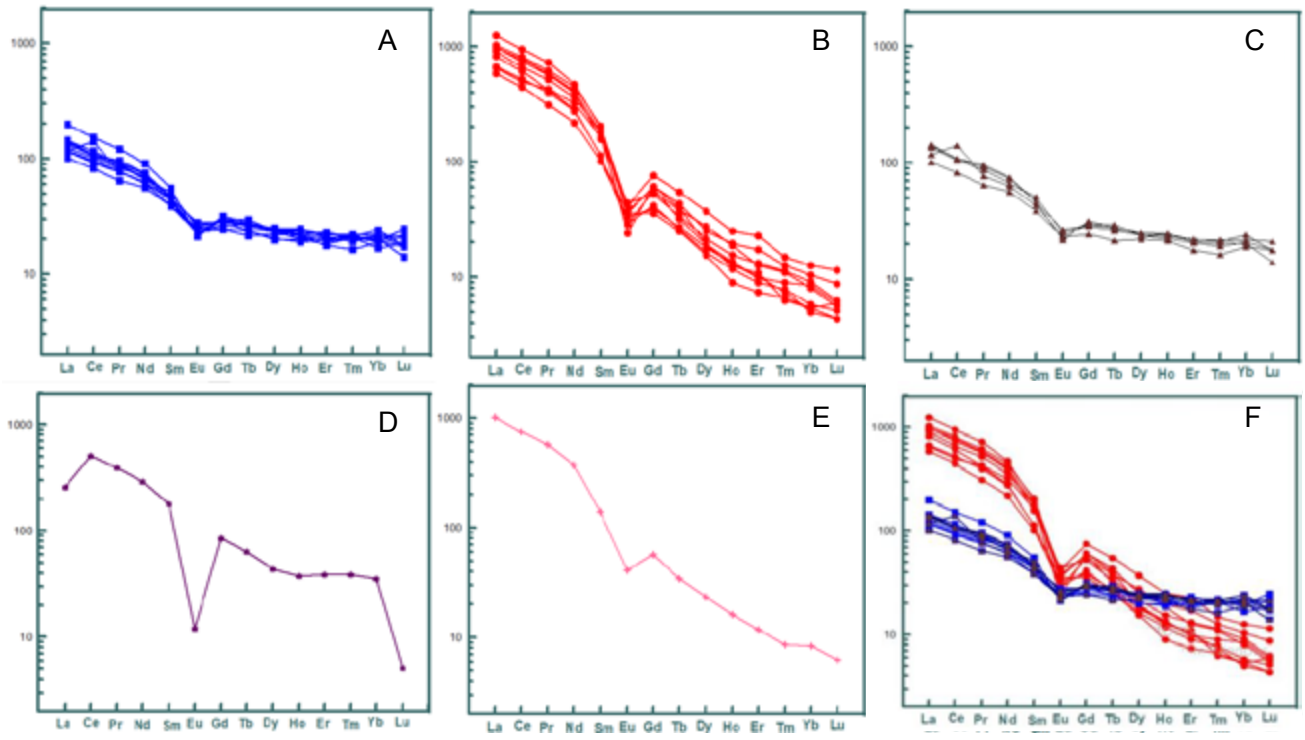

FIGURE 6. Chondrite-normalized REE diagram for: A) migmatitic banded gneisses; B) granitic intrusions; C) garnet mica schist; D) dolerites; E) rhyolite porphyry; F) A, B and C overlap. Values from Sun and McDonough (1991).

melting (Rajesh, 2007; Taylor, 1965). Moreover, the positive correlation of the migmatitic gneisses, schists and granitic intrusions in the Ni *vs.* Cr plot (Fig. 7A) is consistent with partial melting processes. This behavior of the trace elements suggests H_2O-fluxed melting in which plagioclase is the principal reactant, followed by melt extraction. In addition, the LILE and HFSE concentrations indicate a high profile partial melting regime. The fact that the higher ratios of incompatible elements in the granitic intrusions (Rb/Sr= 0.16 to 1.31; Ba/Sr= 0.75 to 6.21) are higher than the ratios in the migmatitic gneisses and schists (Rb/Sr= 0.051 to 0.824; Ba/Sr= 0.7 to 5) lends support to partial melting during crustal anatexis (Rajesh, 2007). The trends during crustal anatexis are also evident in the values of these ratios obtained for the biotite-depleted granitic intrusions with respect to the biotite rich ones. The evolution of the granitic rocks through crustal anatexis is corroborated by the occurrence of plastic deformation in the granitic rocks and in the lenses of melanocratic to mesocratic mica schist which are probably the remnants of the partially melted rocks. Onyeagocha (1986) described rocks similar to the lenses of the micaceous schistose rocks as xenoliths of older schists. This trend is consistent with the one observed in granitic rocks in the southeastern part of the Nigerian Basement Complex by Rahman *et al.* (1988). The depletion in Ba and Sr in the porphyritic rhyolite is evidence of a very late stage of differentiation (Taylor, 1965). On the other hand, the enrichment in Rb in the dolerite could be due to late crystallization of plagioclase feldspars, which is responsible for such a phenomenon in basic igneous rocks (Taylor, 1965).

The abnormally high values of Ni (90) and Cr (120) in the more mafic granitic rocks (garnetiferous biotite granites) are common features of such mafic granitic rocks (Fourcade and Allegre, 1981; Herts and Dutra, 1960; Taylor, 1965). Such enrichment could also come from interactions of melts with the garnet biotite schists. Similarly, high Cr-contents have been recorded in intermediate and ultra-mafic gneisses (Price and Muecke, 1980), as well as in charnockites from southern India (Rajesh, 2007). The enrichment of some of the HFSE in the migmatitic gneisses, schists and granitic intrusions and that of Hf in the porphyritic rhyolite suggest volatile concentrations during the evolution of these rocks. The high level of enrichment in the LREE with respect to the HREE in all the rocks suggests, in general, a high degree of fractionation. This is also evident in the elevated values of the normalized ratios of La to Yb, Ce to Yb and La to Sm which show that the rocks are LREE enriched, the highest values being recorded in the more fractionated granitic intrusions. Light REE enrichment with respect to the heavy REE has been recorded in granitic rocks from other parts of the Precambrian Basement Complex of Nigeria by Onyeagocha (1986), Olarewaju (1987) and

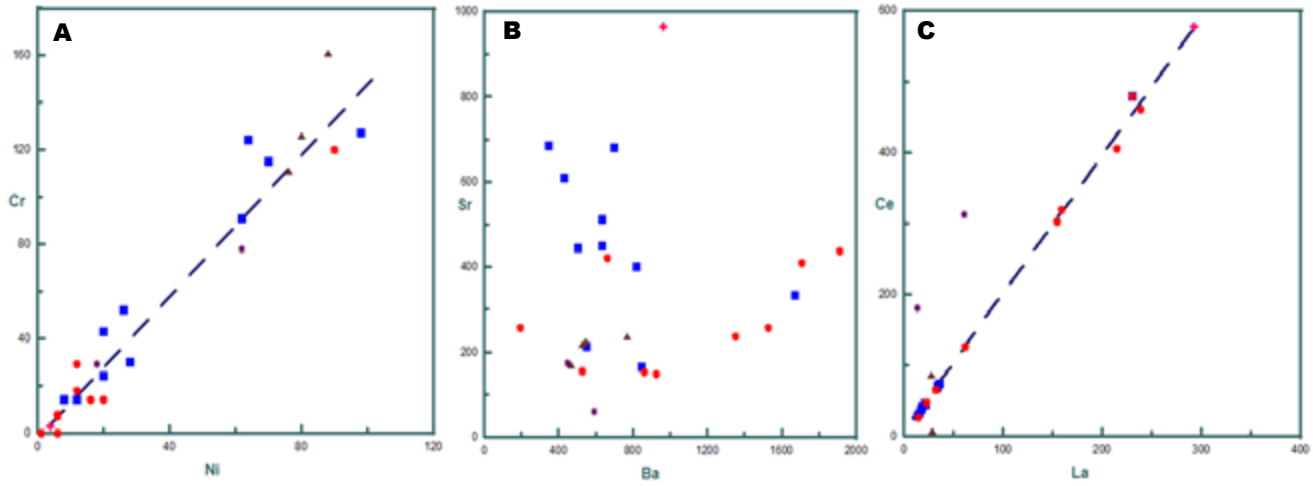

FIGURE 7. Incompatible element ratio diagrams of the basement complex rocks: A) Ni *vs.* Cr, B) Ba *vs.* Sr and C) La *vs.* Ce.

Ukaegbu and Ekwueme (2006). The smooth REE patterns in addition to the negative Eu anomaly shown by the granitic intrusions are common features of granites that are formed by crustal anatexis (Emmermann *et al*., 1975; Ibe and Obiora, 2019). The negative Eu anomalies in the granitic rocks and porphyritic rhyolite show that a high amount of plagioclase was removed from the felsic magma during fractional crystallization (Rollinson, 1993).

An orogenic origin which is most probably post-collisional in character is suggested by the plots of most of the granitic rocks in the field of post-collisional granites as well as in the other fields of orogenic granites in the Rb versus Y+Nb discrimination diagram of Pearce *et al.* (1984) and in the Rb/30-Hf-3Ta ternary diagram of Harris *et al.* (1986). This post-collision orogenic setting is consistent with the result obtained for other Pan-African granites from different parts of the Precambrian Basement Complex of Nigeria (Obiora and Umeji, 1997) and with the plots of orthogneisses, granites and charnockies from Obudu Plateau in the southeastern Precambrian Basement Complex in Nigeria (Ukaegbu and Ekwueme, 2006). The evolution of some of the granitic intrusions in the Precambrian Basement Complex in Nigeria through partial crustal melting has been proposed (Ibe and Obiora, 2019; Obiora, 2005, 2006; Onyeagocha, 1986; Oyawoye, 1964, 1972; Rahman *et al*., 1988). It is believed that the granitic rocks were produced by the reactivation of the internal region of the Pan-African belt during the collision between the active continental margin of the Tuareg shield and the passive margin of the West African craton, about 600Ma ago (Wright, 1985). The granitic rocks were most likely formed towards the end of this Pan-African collision event. Post-collision granites are represented by a mixture of subduction-like mantle sources with the characteristics of volcanic arc granites, intra-plate sources with the attributes of within-plate granites and extensive interactions between the mantle-derived sources and the crust. The within-plate setting displayed by both the dolerite and the porphyritic rhyolite suggests a link with anorogenic magmatism.

CONCLUSIONS

The trace and REE concentrations in the granitic rocks of the Precambrian Basement Complex within the Bamenda massif (southeastern Nigeria) suggest that the granitic intrusions evolved from migmatitic banded gneisses and garnet mica schists during partial melting/crustal anatexis. The granitic rocks are more fractionated. A negative Eu anomaly indicates that plagioclase feldspar was fractionated during anatexis. Enrichments in some of the HFSE suggest volatile concentrations during the evolution of the rocks whereas abnormally high Ni and Cr contents in the granitic intrusions are attributed to a mafic nature (Singh *et al*., 2006). The granitic rocks were formed in an orogenic setting, which is most probably post-collisional. This suggests that the crustal melting occurred towards the end of the collision between the active continental margin of the Tuareg shield and the passive continental margin of the West African craton. This orogenic event is believed to have reactivated the internal region of the Pan-African belt. The dolerite and the porphyritic rhyolite on the other hand were formed in intra-plate settings and are most likely related to the anorogenic Jurassic (Younger) granite magmatism in the eastern part of north central Nigeria.

CONFLICT OF INTEREST

The author hereby declares no conflict of interest.

ACKNOWLEDGMENTS

The author is grateful to the Association of Applied Geochemists for providing in-kind analytical support for the geochemical analysis and also to Smart C. Obiora for proofreading the work and providing his publication to be used as a model for this research. I gratefully acknowledge the constructive and very helpful comments from the anonymous reviewers.

REFERENCES

Anike, O.L., Umeji, A.C., Orajaka, I.P., 1993. Geology of Precambrian Banded Iron formation from Muro Hill, Nigeria. Economic Geology, 88, 1237-124.

Brown, M., 1994. The generation, segregation, ascent and emplacement of granite magma: the Migmatite-to-crustally-derived granite connection in thickened orogens. Earth Science Reviews, 36, 83-130.

Castro, A., Moreno-Ventas, I., De la Rosa, J.D., 1991. H-type (hybrid) granitoids: a proposed revisión of the granite type classification and nomenclature. Earth-science reviews, 31(3-4), 237-253.

Chappell, B.W., 1996. Magma mixing and the production of compositional variation within granite suites: evidence from the granites of southeastern Austrailia. Journal of Petrology, 37(3), 449-470.

Clemens, J.D., 1990. The granulite-granite connection. In: Vielzeuf, D., Vidal, Ph. (eds.). Granulites and crustal evolution. Dordrecht, Kluwer, 25-36.

Cordani, U.G., Pimentel, M.M., Ganade de Araújo, C.E., Basei, M.A.S., Fuck, R.A., Girardi, V.A.V., 2013. Was there an Ediacaran Clymene ocean in central South America? American Journal of Science, 313, 517-539.

Emmermann, R., Daieva, L., Schneider, J., 1975. Petrologic significance of rare earths distribution in granites. Contributions to Mineralogy and Petrology, 52, 267-283.

Floyd, P.A., Winchester, J.A., 1975. Magma type and tectonic setting discrimination using immobile elements. Earth and planetary science letters, 27, 211-218.

Fourcade, S., Allergre, C.J., 1981. Trace elements behaviour in granite genesis: a case study. The calc-alkaline plutonic association from the Quergut Complex (Pyrénées, France). Contributions to Mineralogy and Petrology, 76, 177-195.

Frost, T., Mahood, G.A., 1987. Field, chemical and physical constraints on mafic-felsic magma interaction in the Lamarck Granodiorite, Sierra Nevada, California. Geological Society of America Bulletin, 99(2), 272-291

Harris, N.B.W, Pearce, J.A., Tindle, A.G., 1986. Geochemical characteristics of collision-zone magmatism. Geological Society, London, 19 (1, special publications), 67-81.

Haskin, L.A., Haskin, M.A., Frey, F.A., Wildman, T.R., 1968. Relative and absolute terrestrial abundances of the rare-earths. In: Ahrens, L.A. (ed.). Origin and distribution of elements. Oxford, Pergamon, 1, 889-911.

Hers, N., Dutra, C.V., 1960. Minor element abundance in a part of the Brazillian Shield. Geochimica et Cosmochimica Acta, 21, 81-98.

Ibe, C.U., Obiora, S.C., 2019. Geochemical characterization of Granitoids in Katchuan Irruan area: further evidence for peraluminous and shoshonitic compositions and postcollisional setting of granitic rocks in the Precambrian Basement Complex of Nigeria. Acta Geochimica, 38(5), 734-752.

Ibe, C.U., 2020. Geochemical characterization of the gneisses and schists in Ekumtak area: further evidence for a metasedimentary protolith and moderate weathering intensity for the Precambrian Basement complex of Nigeria. Serie Correlación Geológica, 35(2), 17-36.

Lambert, I.B., Heier, K.S., 1968. Geochemical investigations of deep-seated rocks in the Austrailian shield. Lithos, 1, 30-53.

Malomo, S., 2004. Geological Map of Nigeria, 1:2,000,000. Published by the Nigeria Geological Survey Agency.

Neves, S.P., Vauchez, A., 1995. Successive mixing and mingling of magmas in a plutonic complex of Northeast Brazil. Lithos, 34, 275-299

Nockolds, S.R., Allen, R., 1953. The geochemistry of some igneous rock series. Geochimica et Cosmochimica Acta, 4, 105-142.

Obiora, S.C., Umeji, A.C., 1997. An appraisal of the use of discrimination diagrams in the tectonomagmatic classification of Igneous Rocks in Nigeria. Jos 1997, Annual International Conference of the Nigeria Mining and Geoscience Society, 33 (abstracts), 47.

Obiora, S.C., 2005. Field Description of Hard Rocks, with examples from the Nigeria Basement Complex. Enugu (Nigeria), SNAAP Press Ltd., 44pp.

Obiora, S.C., 2006. Petrology and geotectonic setting of Basement Complex rocks around Ogoja, southeastern Nigeria. Ghana Journal of Science, 46, 13-25.

Obiora, S.C., Ukaegbu, V.U., 2009. Petrology and Geochemistry Characteristics of Precambrian granite Basement Complex rocks in the southernmost part of North Central Nigeria. Chinese Journal of Geochemistry, 28(4), 377-385.

Obiora, S.C., 2012. Chemical characterization and tectonic evolution of Hornblende-Biotite granitoids from the Precambrian basement complex around Ityowanye and Katsina-Ala, Southeastern Nigeria. Journal of mining and Geology, 48, 13-29.

Olarewaju, V.O., 1987. Charnockite – granite association in SW, Nigeria: Rapakivi granite type and charnockitic plutonism in Nigeria? Journal of African Earth Sciences, 6(1), 67-77.

Onyeagocha, A.C., 1986. Geochemistry of basement granitic rock from northcentral Nigeria. Journal of African Earth Sciences, 5(6), 651-657.

Oyawoye, M.O., 1964. The geology of the Nigerian Basement Complex- A survey of our present knowledge of them. Nigerian Mining, Geological and Metallurgical Society, 1, 87-102.

Oyawoye, M.O., 1972. The Basement Complex of Nigeria. In: Dessauvagie, T.F.J., Whiteman, A.J. (eds.). Ibadan, African Geology. Ibadan University Press, 67-99.

Pearce, J., Cann, J.R., 1973. Tectonic setting of basic volcanic rocks determined using trace element analysis. Earth and Planetary Science Letters, 19, 290-300.

Pearce, J.A., Norry, M.J, 1979. Petrogenetic implications of Ti, Zr, Y and Nb variations in volcanic rocks. Contributions to Mineralogy and Petrology, 69, 33-47.

Pearce, J.A., Harris, N.B.W., Tindle, A.G., 1984. Trace element discrimination diagram for the tectonic interpretation of granitic rocks. Journal of Petrology, 25(4), 956-983.

Pearce, J., 1996. Sources and settings of granitic rocks. Episodes, 19(4), 120-125.

Price, C., Mueke, G.K., 1980. Rare-earth geochemistry of the Scourian complex N.W Scotland–Evidence for the granite-granulite link. Contributions to Mineralogy and Petrology, 73, 403-412.

Rahman, A.M.S., Ekwere, S.J., Azmatullah, M., Ukpong, E.E., 1988. Petrology and geochemistry of granitic intrusive rocks from the western part of Oban Massif, Southeastern Nigeria. Journal of African Earth Sciences, 7, 149-157.

Rajesh, H.M., 2007. The petrogenetic characterization of intermediate and silicic charnockites in high-grade terrains: A case study from southern India. Contributions to Mineralogy and Petrology, 154, 591-606.

Rollinson, H.R., 1993. Using geochemical data: Evaluation, Presentation and Interpretation. United Kingdom (UK), Longman, 352pp.

Sawyer, E.W., 1996. Melt segregation and magma flow in migmatites: implications for the generation of granite magmas. Transactions of the Royal Society of Edinburgh: Earth Sciences, 87, 85-94.

Sawyer, E.W., 1998. Formation and evolution of granite magmas during crustal reworking: the significance of diatexites. Journal of Petrology, 39, 1147-1167.

Singh, A.K., Singh, R.K.B, Vallinayagam, G., 2006. Anorogenic acid volcanic rocks in the Kundal area of the Malani Igneous suite, Northwestern India: Geochemical and Petrogenetic studies. Journal of Asian Earth Sciences, 27(4), 544-557.

Sun, S.S., McDonough, W.F., 1991. Chemical and isotopic systematic of oceanic basalts: implication for mantle composition and processes. In: Sunders, A.D., Norry, M.J. (eds.). Magmatic in Oceanic Basins. Geology Society of London, 42 (Special Publications), 313-345.

Taylor, S.R., 1965. The application of trace element data to problems in petrology. Physics and Chemistry of the Earth, 6, 133-213.

Thompson, R.N., 1982. British Tertiary volcanic province. Scottish Journal of Geology, 18, 49-67.

Ugwuonah, E.N., Tsunogae, T., Obiora, S.C., 2017. Metamorphic P-T evolution of garnet staurolite-biotite pelitic schist and amphibolites from Keffi, north central Nigeria: Geothermobarometry, mineral equilibrium modeling and P-T path. Journal of African Earth Sciences, 129, 1-16.

Ukaegbu, V.U., Ekwueme, B.N, 2006. Petrogenesis and geotectonic setting of the Pan African basement rocks in Bamenda massif, Obudu, southeastern Nigeria: Evidence from trace element geochemistry. Chinese Journal of Geochemistry, 25(2), 122-135.

Vielzeuf, D., Clemens, J.D., Pin, C., Moinet, E., 1990. Granites, Granulites and crustal differentiation. In: Vielzeuf, D., Vidal, Ph. (eds.). Granulites and crustal evolution. Dordrecht, Kluwer, 59-85.

Wang, X., Zhou, J., Qui, J and Gao, J. 2004. Geochemistry of Meso-to Neoproterozoic basic to acid rocks from Hunan Province, South China: implications for the evolution of the western Jiangnan orogeny. Precambrian Research. 135. 79-103

Winchester, J.A., Floyd P.A., Chocyk, M., Horbowy, K., Kozdroj, W. 1995. Geochemistry and tectonic environment of Ordovician meta-Igneous rocks in the Rudawy Janowickie Complex, SW Poland. Journal of the Geological Society of London. 152, 105-115.

Wood, D.A., 1980. The application of a Th-Hf-Ta diagram to problems of tectonomagmatic classification and to establishing the nature of crustal contamination of basaltic lavas of the British Tertiary Volcanic Province. Earth and Planetary Science Letters, 50, 11-30.

Wright, J.B., 1985. Geology and Mineral Resources of West Africa. London, George Allen and Unwin, 87pp.

Manuscript received May 2020;
revision accepted October 2020;
published Online December 2020.

APPENDIX I

TABLE I. Trace element concentrations (ppm) in the southeastern basement complex rocks

	MBGn	MBGn	MBGn	MBGn	MBGn	MBGn	MBGn	MBGn	MBGn	MBGn	GMS	GMS	GMS	GMS	GMS
Sc	6.9	6.1	10.2	18.5	12.4	8.6	3.5	12.2	18.4	16.2	21.5	19.4	22.7	22.9	26.4
V	36.7	45.3	72.8	123	76.8	80.3	44	49	146	128	168	149	179	173	173
Cr	14	24	91	124	43	52	14	30	127	115	126	111	120	120	161
Co	18.5	17.5	20.8	26.9	15.8	20.5	10.9	18	23.9	33	30.2	26.2	36.3	29.4	27.9
Ni	12	20	62	64	20	26	8	28	98	70	80	76	90	90	88
Cu	18	18	12	54	4	10	22	94	80	28	12	8	114	58	46
Zn	125	60	50	100	50	50	40	40	120	90	120	105	130	115	130
Rb	238	102	83	91.4	69.4	79.9	35.2	38.7	136	95.7	92.9	85.6	88.1	82.2	137
Sr	334	608	511	444	450	401	685	681	165	213	224	217	156	168	235
Y	32.4	8.6	15.5	34.5	12.2	12.3	8.08	21.6	29.5	33	36.2	36.2	37.1	38.5	37.2
Zr	890	150	176	214	121	199	171	275	240	209	189	176	194	201	230
Nb	40.3	6.47	4.61	16.2	4.24	3.75	1.53	6.11	14.6	10.1	9.7	9.6	9.21	9.99	16.1
Sn	1.4	1.6	1.4	4.8	1.4	1.2	0.8	1.4	1.4	2	2.6	2.2	1.6	1.6	2.6
Sb	0.5	0	0.3	0.4	0.2	0.2	0.1	0.3	0.3	0.1	0.2	0.2	0.3	0.3	0
Cs	0.84	1.46	2.05	3.52	1.89	1.79	0.63	1.94	4.3	4.69	5.23	5.04	4.64	4.49	6.7
Ba	1670	430	635	504	636	818	346	697	849	552	548	528	526	468	767
Hf	22.2	3.4	4.14	5.32	5.2	5.73	4.72	7.36	6.93	6.02	4.95	4.67	5.05	5.94	6.64
Ta	3.07	0.6	0.45	1.22	0.34	0.36	0.09	0.51	0.8	0.83	0.84	0.87	0.89	0.8	1.11
W	216	203	140	90.4	90.8	91.7	68.4	170	53.6	235	161	134	175	126	51
Tl	1.2	0.6	0.4	0.6	0.4	0.4	0.4	0.2	0.8	0.6	0.6	0.4	0.6	0.6	0.8
Pb	27	12	9	10	9	9	6	27	18	17	18	17	12	13	18
Th	68.4	3.12	8.08	12	5.68	5.81	0.38	14.2	18.1	8.25	7.07	7.45	8.12	8.73	9.23
U	2.4	0.84	0.54	2.93	0.63	1.19	0.23	2.95	2.85	2.11	2.13	2.65	2.86	2.7	3.29
Ga	21.8	21.3	17.7	22.2	18.4	18.6	20.8	17.2	24	17.8	20.8	18.1	21.3	21.1	24.5
Y+Nb	72.7	15.07	20.11	50.7	16.44	16.05	9.61	27.71	44.1	43.1	45.9	45.8	46.3	48.5	53.3
Rb/Sr	0.713	0.168	0.162	0.206	0.154	0.199	0.051	0.057	0.824	0.449	0.41	0.39	0.56	0.49	0.58
Ba/Rb	7.017	4.216	7.651	5.514	9.164	10.24	9.83	18.01	6.243	5.768	5.9	6.17	5.97	5.69	5.6
Ba/Sr	5	0.707	1.243	1.135	1.413	2.04	0.505	1.023	5.145	2.592	2.45	2.43	3.37	2.79	3.26

TABLE I. Continued

	PAG	PAG	PMBG	PMBG	PHBG	RHP	WFL	GBG	GBG	SP	DOL	DOL	AV. GR	AV. CRST	AV. DOL	AV. RY
Sc	7.6	4.3	4.3	1.1	5	1.7	7.3	22.7	4.4	0.3	37.1	28.8	5	16	18.7	7
V	39.3	26.1	9.2	3	16	3.5	60.3	179	36	0.9	152	94.7	20	135		
Cr	14	7	8	0	14	3	29	120	18	0	78	29	4	100	313	23
Co	46.7	15.6	21.1	8.3	16.8	24.9	19.9	36.3	23.4	48.4	45.2	41.3	1	25	71.2	
Ni	20	6	6	1	16	4	12	90	12	6	62	18	0.5	75	271	101
Cu	22	16	18	4	26	8	8	114	16	1	1	1	10	55		
Zn	125	95	90	45	75	25	40	130	110	4	120	160	40	70		
Rb	213	242	199	181	192	156	65.4	88.1	206	35.1	429	63.8	150	90	27.5	171
Sr	410	258	152	149	236	196	421	156	438	258	61	174	285	375	356	38
Y	24.9	17.8	17.3	8.44	26.2	22.2	9.96	37.1	16.7	30.6	60.1	66	40	30	17.9	289
Zr	909	753	470	116	507	72.9	114	194	741	56	405	672	180	165	161	2091
Nb	37.7	31.1	31.7	11.6	27.9	7.44	4.1	9.21	28.3	1.17	43.8	79.2	30	32		
Sn	1.8	1.2	1.4	1.2	2.2	1	1.2	1.6	2.2	0.6	4.8	2.6	3	2		
Sb	0.2	0.3	0	0.2	0.1	0.3	0.2	0.3	0.2	0.2	0	0.3	0.2	0.2		
Cs	2.76	0.75	1.37	1.68	0.52	0.67	1.43	4.64	1.59	0.46	16.5	1.39	5	3		
Ba	1710	1530	860	926	1350	965	661	526	1910	193	593	450	600	425	1018	141
Hf	22.8	19.4	14.3	3.99	14.9	2.63	2.9	5.05	16.6	2.14	11.5	15.6	4	3	3.49	
Ta	3	1.54	1.11	0.63	1.1	1.11	0.54	0.89	1.61	1.1	2.52	4.71	3.5	2	1.66	
W	1010	221	237	155	260	549	152	175	285	837	44.4	94.8	2	1.5		
Tl	1	1.2	1	1	1.4	1	0.4	0.6	1.2	0.3	2.6	0.4	0.75	0.45		
Pb	22	25	26	35	27	40	9	12	25	29	12	4	20	12.5		
Th	55.3	35.1	53.1	30.4	48.2	20.2	4.52	8.12	47.8	3.75	79.3	6.11	17	10	4.27	34
U	2.23	1.21	1.85	2.69	1.49	3.09	0.78	2.86	1.68	2.54	9.47	2.9	4.8	2.7	0.7	
Ga	21.5	19.6	21.9	15.6	19.9	14.8	17.4	21.3	22.9	18.3	35.3	21.2	18	15		
Y+Nb	62.6	48.9	49	20	54.1	29.6	14.1	46.3	45	31.8	104	145.2				
Rb/Sr	0.52	0.94	1.31	1.21	0.81	0.8	0.16	0.56	0.47	0.14	7.03	0.367	0.53	0.24	0.08	4.5
Ba/Rb	8.028	6.32	4.32	5.12	7.03	6.19	10.1	5.97	9.27	5.5	1.38	7.053	4	4.72	37.02	0.82
Ba/Sr	4.171	5.93	5.66	6.21	5.72	4.92	1.57	3.37	4.36	0.75	9.72	2.586	2.11	1.13	2.86	3.71

TABLE II. REE concentrations (ppm) in the southeastern basement complex rocks

	MBGn	MBGn	MBGn	MBGn	MBGn	MBGn	MBGn	MBGn	MBGn	MBGn	GMS	GMS	GMS	GMS	GMS
La	231	21.9	15.6	14.1	36.3	34.5	18.5	21.5	22.5	17.5	28.7	27.8	32	33.8	33.6
Ce	479	45.5	32.2	28.1	73.6	71.2	41.2	46.1	44.1	37	7.4	86.8	64.8	66.8	66.4
Pr	55.9	5.79	55.2	3.36	8.55	8.54	4.6	5.07	5.91	4.81	7.77	7.31	8.31	9.05	8.77
Nd	191	21.4	15.8	12.1	31.2	31.8	17.3	18.8	23.9	21.4	30.5	29.5	31.1	35.2	34.1
Sm	27.7	4.6	2.95	2.36	5.36	6.53	3.23	3.23	4.13	3.72	6.65	6.6	7.85	7.12	7.09
Eu	2.08	1.04	0.97	0.63	1.19	1.29	1	0.9	0.98	1.34	1.36	1.37	1.48	1.27	1.55
Gd	12.6	3.32	2.44	1.34	3.28	5.6	2.52	2.16	2.9	2.24	5.05	6.09	6.12	6.48	5.93
Tb	1.63	0.41	0.37	0.21	0.51	0.91	0.42	0.43	0.43	0.3	1	1.1	1.02	1.04	0.98
Dy	6.34	1.87	2.2	1.16	2.82	5.93	0	2.2	2.28	1.31	6.04	6.04	6.33	6.08	6.1
Ho	1.11	0.3	0.34	0.22	0.54	1.23	0.13	0.35	0.51	0.43	1.26	1.27	1.4	1.37	1.33
Er	2.88	0.78	1.26	0.59	1.34	3.18	0.54	1.18	1.25	0.67	3.74	3.4	3.46	3.62	3.67
Tm	0.32	0.09	0.1	0.09	0.22	0.52	0.2	0.16	0.14	0.04	0.58	0.49	0.53	0.56	0.54
Yb	1.78	0.52	0.21	1.37	1.76	3.65	0.15	1.06	0.52	0.86	3.39	3.56	3.48	3.71	4.09
Lu	0.22	0.04	0.12	0.07	0.2	0.54	0.13	0.16	0.19	0.12	0.54	0.46	0.36	0.54	0.45
∑REE	1014	108	130	65.7	167	175	89.9	103	110	91.7	104	182	168	177	175
∑LREE	985	99.2	122	60	155	153	84.8	94.7	101	84.4	81	158	144	152	150
∑HREE	26.9	7.33	7.04	5.05	10.7	21.6	4.09	7.7	8.22	5.97	21.6	22.4	22.7	23.4	23.1
∑LREE/HREE	36.6	13.5	17.3	11.9	14.5	7.08	20.7	12.3	12.2	14.1	3.75	7.05	6.35	6.49	6.49
LA_N/Yb_N	93.1	30.2	53.3	7.38	14.8	6.78	88.5	14.5	31	14.6	6.07	5.6	46.4	6.53	5.89
Ce_N/Yb_N	74.8	24.3	42.6	5.7	11.6	5.42	76.3	12.1	23.6	12	0.61	6.77	33.9	5	4.51
La_N/Sm_N	5.38	3.07	3.41	3.86	4.37	3.41	3.7	4.3	3.52	3.04	2.79	2.72	3.81	3.06	3.06
La_N/Lu_N	113	58.7	13.9	21.6	19.5	6.85	15.3	14.4	12.7	15.6	5.7	6.48	6.27	6.71	8
Eu/Eu*	0.34	0.81	1.11	1.08	0.87	0.65	1.07	1.04	0.87	1.42	0.72	0.66	1.19	0.57	0.73

TABLE II. Continued

	PAG	PAG	PMBG	PMBG	PHBG	RHP	WFL	GBG	GBG	PG	Dol	Dol
La	239	159	215	61.6	155	293	22.9	32	14.5	231	61.3	14.3
Ce	461	320	406	126	303	578	47	64.8	26.8	479	313	180
Pr	54.3	37.8	49.3	14.9	40.5	69.7	6.25	8.31	2.91	55.9	37.4	23.6
Nd	175	129	168	51.5	150	220	24.3	31.1	10.5	191	136	97
Sm	21.3	17.3	27.3	9.68	25.2	29.9	5.93	7.85	1.87	27.7	27.4	19
Eu	2.39	1.68	1.4	1.06	1.66	2.18	1.38	1.48	1.87	2.08	0.7	3.93
Gd	11.7	8.57	12.6	5.22	11.4	12.11	5.83	6.12	1.02	12.6	17.6	15.3
Tb	1.29	0.98	1.49	0.64	1.44	1.2	0.93	1.02	0.45	1.63	2.4	2.27
Dy	5.91	4.13	4.93	2.44	6.99	4.82	5.37	6.33	4.17	6.34	11.1	11.6
Ho	0.91	0.67	0.76	0.33	1.06	0.7	1.21	1.4	1.27	1.11	2.13	2.38
Er	1.94	1.48	1.65	0.55	2.08	1.79	3.3	3.46	5.42	2.88	6.38	6.66
Tm	0.22	0.2	0.19	0.06	0.28	0.16	0.55	0.53	1.12	0.32	0.99	0.84
Yb	1.43	0.98	0.84	0.31	1.37	0.92	1.08	3.48	8.63	1.78	5.99	5.23
Lu	0.16	0.13	0.11	0.04	0.14	0.11	0.45	0.36	0.46	0.22	0.13	0.46
∑REE	976.6	681.9	889.6	274.33	700.1	1215	126.48	168.2	80.99	1014	622.5	382.6
∑LREE	950.6	663.1	865.6	263.68	673.7	1191	106.38	144.1	56.58	984.6	575.1	323.5
∑HREE	23.56	17.14	22.57	9.59	24.76	21.81	18.72	22.7	22.54	26.88	15.62	15.57
∑LREE/HREE	40.35	38.69	38.35	27.495	27.21	54.59	5.6827	6.346	2.51	36.63	36.82	20.78
LA_N/Yb_N	119.9	116.4	183.6	142.53	81.15	228.4	15.209	6.596	1.205	93.09	7.341	1.961
Ce_N/Yb_N	89.55	90.7	134.3	112.9	61.44	174.5	12.088	5.172	0.863	74.75	14.51	9.56
La_N/Sm_N	7.244	5.933	5.084	4.1082	3.971	6.326	2.493	2.632	5.006	5.384	1.444	0.486
La_N/Lu_N	160.1	131.1	209.5	165.05	118.7	285.5	5.4539	9.526	3.378	112.5	50.54	3.332
Eu/Eu*	0.463	0.422	0.231	0.4559	0.299	0.35	0.7175	0.653		0.34	0.097	0.705